Liquid Crystals
Publication details, including instructions for authors and subscription information:
http://www.informaworld.com/smpp/title~content=t713926090

Back-flow and flow-alignment in pulsatile flows of Leslie-Ericksen liquid crystals

L. R. P. de Andrade Lima[a]; A. D. Rey[a]
[a] Department of Chemical Engineering, McGill University, Montreal, QC, Canada H3A 2B2

To cite this Article Lima, L. R. P. de Andrade and Rey, A. D.(2006) 'Back-flow and flow-alignment in pulsatile flows of Leslie-Ericksen liquid crystals', Liquid Crystals, 33: 6, 711 — 722
To link to this Article: DOI: 10.1080/02678290600703973
URL: http://dx.doi.org/10.1080/02678290600703973

Liquid Crystals, Vol. 33, No. 6, June 2006, 711–722

Back-flow and flow-alignment in pulsatile flows of Leslie–Ericksen liquid crystals

L.R.P. DE ANDRADE LIMA and A.D. REY*

Department of Chemical Engineering, McGill University, 3610 University Street, Montreal, QC, Canada H3A 2B2

(*Received 3 November 2005; in final form 23 February 2006; accepted 21 March 2006*)

Analytical solutions to the capillary pulsatile flow of Leslie–Ericksen liquid crystals under small pressure drops are presented, when the imposed small pressure drop contains a steady and a time-periodic contribution. The results show that pulsatile flows initiate periodic back-flows (reorientation-induced flow) which are directly linked to flow-alignment characteristics of the material. The experimentally measurable power requirement (flow rate × pressure drop) is shown to be well suited to quantify back-flows and flow-alignment material properties. The analysis reveals that power requirements deviate from the Newtonian limit when the frequency of the oscillating pressure drop is close to the splay orientation diffusivity, and backflows become significant. In the terminal zone (small frequencies) the response is Newtonian and the power requirement is a quadratic function of amplitude. At large frequencies, the amplitude of back-flow effects saturates and the power requirement is proportional to the square of the alignment viscosity coefficient α_3. An experimental procedure to measure the flow-alignment viscosity coefficient α_3 is formulated, based on large frequency measurements, and a formula derived from the close-form solution to the Leslie–Ericksen equations for capillary pulsatile flows.

1. Introduction

Rheological characterization of liquid crystals is important in the processing of liquid crystals for structural applications and the use of liquid crystals in display applications [1, 2]. Rheological characterization usually employs linear and non-linear steady, transient, and oscillatory flows [2, 3]; here linearity refers to orientation changes due to the imposed flow deformations. The flow geometries of use in rheology are parallel plates, cone-and-plate, capillaries, to name a few [3, 4]. The use of each of these flows for rheological characterization entails significant practical issues, including edge effects, entry losses and free surface instabilities [5]. In this paper we focus on linear pulsatile capillary flow, and show how this relatively simple geometry allows one to detect important rheological information in a simple manner. Pulsatile flows are characterized by the superposition of a steady pressure drop and an oscillatory pressure drop component, which creates a flow and orientation periodic disturbance on the steady flow orientation. From a fundamental point of view, pulsatile flows of liquid crystals give rise to a flow type were the essential features of liquid crystallinity, such as anisotropic viscoelasticity and backflow processes [2], are clearly manifested; here backflow refers to reorientation-induced flow, and is the inverse of flow-induced orientation.

A most significant temperature sensitive rheological property is the shear-flow-aligning characteristics of uniaxial rod-like nematics, which is set by the sign and magnitude of the Leslie viscosity coefficient α_3; for the aligning regime ($\alpha_3>0$), the average molecular orientation or director vector (**n**), is close to the flow direction, while in the non-alignment regime ($\alpha_3<0$), the steady state orientation is non-planar and non-homogeneous [3, 6, 7]. Some nematic liquid crystals (NLCs), such as 8CB, exhibit flow-aligning behaviour if the temperature is sufficiently high but at lower temperatures are non-aligning. At the flow aligning/non-aligning transition temperature ($T_{a\text{-}n}$) the viscosity coefficient α_3 is equal to zero.

Next we describe the proposed rheological technique that motivates this theoretical paper based on the Leslie–Ericksen model [8–12]. Flow alignment has a direct impact on back-flow, when the director is aligned along the flow direction. As is well known, the contribution of back-flow B to the momentum equation in the linear regime is [8–12]:

$$B = -\alpha_3 \frac{\partial \theta}{\partial t} \tag{1}$$

*Corresponding author. Email: alejandro.rey@mcgill.ca

Liquid Crystals
ISSN 0267-8292 print/ISSN 1366-5855 online © 2006 Taylor & Francis
http://www.tandf.co.uk/journals
DOI: 10.1080/02678290600703973

where θ is the small deviation of the director angle with respect to the flow direction. Furthermore, the director velocity $\partial\theta/\partial t$ is given by the sum of an elastic contribution ($\Sigma(\bigtriangledown\theta)$) and a pressure drop contribution ($\alpha_3\Delta P$):

$$\frac{\partial\theta}{\partial\widetilde{T}} = \Sigma(\nabla\theta) + \alpha_3\Delta P \tag{2}$$

the latter being introduced by α_3; $\bigtriangledown\theta$ denote spatial gradients and ΔP is proportional to the pressure drop. Hence the director velocity is a function of α_3 and the strength of back-flow may be written:

$$B \propto (\alpha_3)^2 \tag{3}$$

thus connecting flow-alignment to back-flow. The next link into the rheological technique is the relation between back-flow and flow rate. As mentioned above, the pulsatile flow has a steady and an oscillatory velocity component. The oscillatory component is due to transient oscillations and back-flow. Hence the total flow rate will have a steady and a back-flow contribution:

$$Q = Q_{\text{steady}} + Q_{\text{back}-\text{flow}} \tag{4}$$

where according to equations (3) and (4): $Q_{\text{back}-\text{flow}} \propto \alpha_3^2$. Finally, measuring the pumping power W ($W = Q \times \Delta P$), gives direct information on the magnitude of α_3^2. In this paper we focus on 4-*n*-octyl-4′-cyanobiphenyl (8CB), which has well characterized viscoelastic parameters and an aligning/non-aligning rheological transition at $T = 38.36^{\circ}$C; this transition has been the subject of many studies [2, 7, 13]. The Leslie–Ericksen model has been shown to capture most if not all rheological features of 8CB [7, 14, 15] and is well suited for most low molar mass NLCs far from phase transition regions, when order parameter processes have significant impact on flow-processes.

The objectives of this paper are: (1) to characterize the role of back-flow and flow-alignment in pulsatile flow of NLCs by solving the Leslie–Ericksen nematodynamics equations; (2) to characterize the relationship between power requirements and flow-alignment in pulsatile flows of NLCs; (3) to propose a rheological procedure to assess the magnitude of α_3 by measuring pumping power.

This paper is organized as follows. Section 2 presents the governing equations and auxiliary data to describe the NLCs pulsatile capillary Poiseuille flow. Section 3 presents the analytical results and discussions for the pulsatile capillary Poiseuille flow in the linear viscoelastic regime. Section 4 presents the conclusions.

2. Theory and governing equations

2.1. *Leslie-Ericksen equations*

Flowing liquid crystal systems generate elastic and viscous stresses and torques. The elastic energy arises from spatial gradients in the average orientation and to lowest order is given by the Frank energy density F_{d} [1, 16]:

$$2F_{\text{d}} = K_{11}(\nabla\cdot\mathbf{n})^2 + K_{22}(\mathbf{n}\cdot\nabla\times\mathbf{n})^2 + K_{33}|\mathbf{n}\times\nabla\times\mathbf{n}|^2 \tag{5}$$

where K_{11}, K_{22} and K_{33} are the splay, twist and bend temperature–dependent elasticity moduli.

The Leslie–Ericksen continuum theory of flowing uniaxial NLCs is given by the linear momentum balance equation and the internal angular momentum balance equation. The orientation is defined by the director **n** that is a unit vector collinear with the average molecular orientation direction, as shown in figure 1. For incompressible and isothermal conditions the momentum balances are:

$$\rho\left(\frac{\partial v}{\partial t} + \mathbf{v}\cdot\nabla\mathbf{v}\right) = \mathbf{f} + \nabla\cdot\boldsymbol{\tau} \tag{6}$$

$$\rho_1\ddot{\mathbf{n}} = \mathbf{G} + \mathbf{g} + \nabla\cdot\boldsymbol{\pi} \tag{7}$$

where ρ is the density, **v** is the velocity, **f** is the body force per unit volume, $\boldsymbol{\tau}$ is the total stress, ρ_1 is the moment of inertia per unit volume, **G** is the external director body force, **g** is the intrinsic director body force, and $\boldsymbol{\pi}$ is the director stress tensor.

The constitutive equations are:

$$\boldsymbol{\tau} = -p\mathbf{I} - \frac{\partial F_{\text{d}}}{\partial\nabla\mathbf{n}}\cdot\nabla\mathbf{n}^{\text{T}} + \alpha_1(\mathbf{nn}:\mathbf{A})\mathbf{nn} + \alpha_2\mathbf{nN} + \alpha_3\mathbf{Nn} + \alpha_4\mathbf{A} + \alpha_5\mathbf{nn}\cdot\mathbf{A} + \alpha_6\mathbf{A}\cdot\mathbf{nn} \tag{8}$$

$$\mathbf{g} = a\mathbf{n} - \boldsymbol{\beta}\cdot\nabla\mathbf{n} - \frac{\partial F_{\text{d}}}{\partial\mathbf{n}} - \gamma_1\mathbf{N} - \gamma_2\mathbf{n}\cdot\mathbf{A} \tag{9}$$

$$\boldsymbol{\pi} = \boldsymbol{\beta}\mathbf{n} + \frac{\partial F_{\text{d}}}{\partial\nabla\mathbf{n}} \tag{10}$$

$$2\mathbf{A} = \nabla\mathbf{v} + \nabla\mathbf{v}^{\text{T}}; \quad 2\mathbf{W} = \nabla\mathbf{v} - \nabla\mathbf{v}^{\text{T}}; \quad \mathbf{N} = \dot{\mathbf{n}} - \mathbf{W}\cdot\mathbf{n} \tag{11a,b,c}$$

$$\gamma_1 = \alpha_3 - \alpha_2; \quad \gamma_2 = \alpha_6 - \alpha_5 = \alpha_3 + \alpha_2 \quad \lambda = -\gamma_2/\gamma_1 \tag{12a,b,c}$$

where p is the pressure, **I** is the unit tensor, $\{\alpha_i\}$, $i = 1\ldots6$, are the six Leslie viscosity coefficients, **A** is the rate of deformation tensor, **N** is the corotational derivative of the director, $\boldsymbol{\beta}$ and a are respectively an arbitrary vector and an arbitrary scalar used to constrain the director (**n**) to be a unit vector, γ_1 is the rotational viscosity, γ_2 is the irrotational torque coefficient, **W** is the vorticity tensor

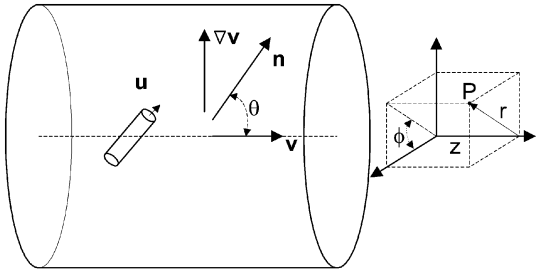

Figure 1. Capillary flow of a uniaxial rod-like nematic liquid crystal, show the unit normal vector (**u**), the director vector (**n**), the velocity vector (**v**), the velocity gradient (∇**v**), the alignment angle (θ) and the cylindrical (r, ϕ, z) coordinate system used to describe a generic point P. Under pressure drop oscillations the director oscillates around $\mathbf{n}_o=(0, 0, 1)$.

and λ is the reactive parameter. The Leslie viscosity coefficients are linked by equation (12*b*) and by four inequalities arising from thermodynamic restrictions [1, 16].

The inertial term in the linear momentum balance equation (6) and the director inertia in equation (7) are both neglected; the former is because the velocity field evolves much faster than the orientation field, so the velocity relaxation time is irrelevant with respect to the orientation relaxation time [1]; the latter is because it is insignificant in comparison with the retained viscous terms.

2.2. *Leslie-Ericksen equations for transient capillary Poiseuille flow*

Consider a small-amplitude oscillatory Poiseuille capillary flow of a nematic liquid crystal, driven by pressure drop oscillations of infinitesimal amplitude, as shown in figure 1, in which the cylindrical coordinate system is also defined. The flow is described by an axisymmetric oscillatory planar director field ($\mathbf{n}(r, t)=(\sin\theta(r, t), 0, \cos\theta(r, t))$), and a purely axial oscillatory velocity field ($\mathbf{v}(r, t)=(0, 0, v(r, t))$) with finite velocity gradient at the centreline. Linearizing around the axial direction (i.e. $\sin\theta\cong\theta$, $\cos\theta\cong1$), the dimensionless governing equations for the director tilt angle $\theta(\tilde{r}, \tilde{t})$ and the axial velocity $\tilde{v}(\tilde{r}, \tilde{t})$ simplify to [8–12]:

$$\tilde{\eta}_{\text{splay}}\frac{\partial\theta}{\partial\tilde{t}}=\frac{\partial}{\partial\tilde{r}}\left[\frac{1}{\tilde{r}}\frac{\partial}{\partial\tilde{r}}(\tilde{r}\theta)\right]+\frac{\tilde{\alpha}_3}{2\tilde{\eta}_1}E\tilde{r} \tag{13}$$

$$\frac{\partial\tilde{v}}{\partial\tilde{r}}=-\frac{E\tilde{r}}{2\tilde{\eta}_1}+\tilde{B} \tag{14}$$

$$\tilde{B}=-\frac{\tilde{\alpha}_3}{\tilde{\eta}_1}\frac{\partial\theta}{\partial\tilde{t}} \tag{15}$$

$$\tilde{\eta}_{\text{splay}}=\tilde{\gamma}_1-\frac{\tilde{\alpha}_3^2}{\tilde{\eta}_1}=\tilde{\gamma}_1\left[1-\frac{\tilde{\gamma}_1}{4\tilde{\eta}_1}(1-\lambda)^2\right] \tag{16}$$

where $\tilde{\eta}_{\text{splay}}$ is the dimensionless splay viscosity, $\tilde{\alpha}_i$ are the dimensionless Leslie viscosities ($\tilde{\alpha}_i=\tilde{\alpha}_i/\langle\eta\rangle$), $\langle\eta\rangle$ is the average Miesowicz viscosity [16], $E(\tilde{\omega}\tilde{t})=\frac{R^3}{K_{11}}\left(-\frac{\mathrm{d}p}{\mathrm{d}z}(\tilde{\omega}\tilde{t})\right)$ is the ratio of viscous flow effects to long range elasticity effects known as the Ericksen number, $\tilde{r}=r/R$ is the dimensionless radius, R is the capillary radius, $\tilde{t}=K_{11}t/\left(R^2\langle\eta\rangle\right)$ is the dimensionless time, $\tilde{v}=\langle\eta\rangle Rv/K_{11}$ is the scaled axial velocity, $-\mathrm{d}p/\mathrm{d}z$ is the given small amplitude oscillatory pressure drop in the capillary per unit length, $\tilde{\omega}=\omega\left(R^2\langle\eta\rangle\right)/K_{11}$ is the dimensionless frequency, and B is the back-flow [8–12].

The boundary conditions for the director orientation angle represent strong planar anchoring, $\theta(0,\tilde{t})=\theta(1,\tilde{t})=0$, and for the axial velocity the no slip condition at the bounding surface is used, $\tilde{v}(1,\tilde{t})=0$. The director oscillates around the velocity (z) direction, and the undistorted director field is given by: $\mathbf{n}_o=(0, 0, 1)$, or perfectly aligned along the flow direction.

For the small amplitude oscillatory capillary Poiseuille flow considered in this paper, the Ericksen number (i.e. dimensionless pressure drop) oscillates as follows:

$$E=E_0(1+A\sin\tilde{\omega}\tilde{t}) \tag{17}$$

where E_o is the average Ericksen number, A is the amplitude, and $\tilde{\omega}$ is the dimensionless frequency. The frequency $\tilde{\omega}$ is scaled with the orientation time scale $\tau_o=(R^2\langle\eta\rangle)/K_{11}$ and the maximum elastic storage is expected for frequencies close to the reciprocal of this value.

2.3. *Material properties*

The viscoelastic material properties needed to characterize the impact of flow-alignment on pulsatile flow of NLCs, when the director is aligned along the capillary axis, includes the Miesowicz viscosities η_1, the torque coefficient α_3, and the reorientation viscosity η_{splay} [1, 16]. Here we give a basic discussion of well known results [1, 8–12, 16].

The Miesowicz shear viscosities that capture the viscous anisotropy of liquid crystals are measured in a steady simple shear flow between parallel plates with fixed director orientations along three characteristic orthogonal directions: (1) $\eta_1=(\alpha_3+\alpha_4+\alpha_6)/2$ when the director is parallel to the velocity direction; (2) $\eta_2=(-\alpha_2+\alpha_4+\alpha_5)/2$ when it is parallel to the velocity

gradient; and (3) $\eta_3=\alpha_4/2$ when it is parallel to the vorticity axis. The measured Miesowicz shear viscosities for aligning nematics usually follow the ordering:

$$\eta_2 > \eta_3 > \eta_1. \tag{18}$$

In the present flow η_1 is the relevant steady shear viscosity, but the average of the three Miesowicz viscosities is used for scaling proposes.

The shear flow alignment of rod-like NLCs is governed by the magnitude of the reactive parameter viscosity coefficient $\alpha_3(T)$. For rods the inequality $\alpha_2<0$ holds at all temperatures, but α_3 may change sign. For rod-like molecules, when $\alpha_3<0$ the material is known as shear flow-aligning, and the director aligns within the shear plane, at an angle θ_L, known as the flow-alignment Leslie angle, given by [1, 16]:

$$\theta_L = \frac{1}{2}\cos^{-1}\left(\frac{1}{\lambda}\right). \tag{19}$$

In a steady simple shear flow when the director is aligned along θ_L the viscous torques are zero. The Leslie angle can be measured using optical methods. When $\alpha_3>0$, non-aligning behaviour arises and equation (19) does not hold.

The transient director reorientation is a viscoelastic process, and the reorientation viscosities associated with splay, twist, and bend deformations are defined by [1, 8]:

$$\eta_{twist} = \gamma_1 \tag{20}$$

$$\eta_{splay} = \gamma_1 - \frac{\alpha_3^2}{\eta_1} \tag{21}$$

$$\eta_{bend} = \gamma_1 - \frac{\alpha_2^2}{\eta_2}. \tag{22}$$

These viscosities are given by the rotational viscosity (γ_1) decreased by a factor introduced by the back-flow effect. Back-flow is a reorientation-driven flow and is essentially the reverse effect to flow-induced orientation. The general expression for the reorientation viscosities can be rewritten as $\eta_\alpha=\gamma_1-(TC_i)^2/\eta_i$, where η_i denotes the corresponding Miesowicz viscosity and TC_i the corresponding torque coefficient. Since twist is the only mode that creates no back-flow then $\eta_{twist}=\gamma_1$. For a bend distortion the back-flow is normal to **n** and hence the torque coefficient is α_2, and the Miesowicz viscosity is η_2. On the other hand for a splay distortion the back-flow is parallel to **n** and hence the torque coefficient is α_3, and the Miesowicz viscosity is η_1. In the present flow the relevant reorientation viscosity is $\eta_{splay}=\gamma_1-\alpha_3^2/\eta_1$. For a material like 8CB, the splay viscosity is a minimum at the aligning/non-aligning transition.

In this paper we use the viscoelastic material parameters of 8CB, shown in table 1 [17, 18]. At a temperature $T=T_{a\text{-}n}=38.5^\circ$C, the viscosity coefficient $\alpha_3=0$. As mentioned above for temperatures above $T_{a\text{-}n}$, $\alpha_3<0$ and flow-alignment is observed, while for temperatures below $T_{a\text{-}n}$, $\alpha_3>0$ and non-alignment is observed. In this paper we discuss results in terms of α_3.

2.4. *Power requirement*

Under steady pressure drop, the dimensionless steady state flow rate $\widetilde{Q}_s(Er_o)$ is given by:

$$\widetilde{Q}_s(Er_o) = 2\pi \int_0^1 \widetilde{v}_s(\widetilde{r}, Er_o)\widetilde{r}\,d\widetilde{r} \tag{23}$$

and the corresponding dimensionless apparent steady viscosity $\widetilde{\eta}_{app,s}(Er_o)$ is:

$$\widetilde{\eta}_{app,s}(Er_o) = \frac{\pi\, Er_o}{8\,\widetilde{Q}_s(Er_o)}. \tag{24}$$

In pulsatile flow, the time-periodic instantaneous dimensionless flow rate $\widetilde{Q}(t)$ is:

$$\widetilde{Q}\left(\widetilde{T}\right) = 2\pi \int_0^1 \widetilde{v}\widetilde{r}\,d\widetilde{r} \tag{25}$$

where $\widetilde{v}$ is the instantaneous velocity. The time-averaged dimensionless flow rate $\langle\widetilde{Q}\rangle$ is:

$$\langle\widetilde{Q}\rangle = \frac{2\pi}{\widetilde{\tau}}\int_0^{\widetilde{\tau}}\left(\int_0^1 \widetilde{v}\widetilde{r}\,d\widetilde{r}\right)du, \quad \widetilde{\tau} = \frac{2\pi}{\widetilde{\omega}} \tag{26}$$

and $\widetilde{\tau}$ is the cycle period of the pressure wave.

The power requirement per unit length to pump a fluid is given by the product of the flow rate and the pressure drop. The instantaneous power requirement to pump a fluid using pulsating flow is given by [4, 19, 20]:

$$\widetilde{W}(\widetilde{t}) = \widetilde{Q}(\widetilde{t})Er(\widetilde{t}). \tag{27}$$

The ratio between the power requirement to pump a fluid using pulsating flow to steady flow is given by:

$$P = \frac{\langle\widetilde{W}\rangle}{\widetilde{W}_s} \tag{28}$$

where the dimensionless steady power requirement $\widetilde{W}_s$ is given by:

$$\widetilde{W}_s = \widetilde{Q}_s\, Er_o \tag{29}$$

Table 1. Viscosity coefficients of 4-*n*-octyl-4′-cyanobiphenyl (8CB) [17, 18].

Set	1	2	3	4[a]	5	6	7
T/°C	34.00	35.00	37.00	38.36	39.00	40.00	40.50
Leslie viscosities coefficients/Pa s							
α_1	0.6510	0.1342	0.0382	0.0196	0.0138	0.0078	0.0060
α_2	−0.0707	−0.0696	−0.0587	−0.0500	−0.0458	−0.0371	−0.0305
α_3	0.0404	0.0140	0.0031	0.0000	−0.0011	−0.0034	−0.0055
α_4	0.0582	0.0560	0.0520	0.0497	0.0488	0.0478	0.0474
α_5	0.0644	0.0529	0.0472	0.0415	0.0388	0.0339	0.0315
α_6	0.0341	−0.0026	−0.0084	−0.0085	−0.0082	−0.0067	−0.0046
Reactive parameter							
λ	0.2725	0.6639	0.9013	1.0000	1.0512	1.2042	1.4436
Dimensionless Leslie viscosities coefficients ($\tilde{\alpha}_1 = \alpha_1/\langle\eta\rangle$)[b]							
$\tilde{\alpha}_1$	10.166	2.6671	0.8932	0.5067	0.3735	0.2291	0.1855
$\tilde{\alpha}_2$	−1.1044	−1.3832	−1.3725	−1.2925	−1.2395	−1.0896	−0.9428
$\tilde{\alpha}_3$	0.6309	0.2782	0.07249	0.0000	−0.02978	−0.09985	−0.1700
$\tilde{\alpha}_4$	0.9089	1.1130	1.2159	1.2848	1.3207	1.4038	1.4652
$\tilde{\alpha}_5$	1.0057	1.0513	1.1037	1.0728	1.0501	0.9956	0.9737
$\tilde{\alpha}_6$	0.5325	−0.05167	−0.1964	−0.2197	−0.2219	−0.1968	−0.1422
Dimensionless rotational viscosity and irrotational torque coefficient							
$\tilde{\gamma}_1$	1.7350	1.6615	1.4450	1.2925	1.2097	0.9897	0.7728
$\tilde{\gamma}_2$	−0.4732	−1.1050	−1.3001	−1.2925	−1.2693	−1.1894	−1.1128
Dimensioneless Miesowicz viscosities							
$\tilde{\eta}_1$	1.0362	0.6698	0.5460	0.5325	0.5345	0.5536	0.5765
$\tilde{\eta}_2$	1.5094	1.7738	1.8461	1.8251	1.8051	1.7445	1.6909
$\tilde{\eta}_3$	0.4544	0.5565	0.6080	0.6424	0.6604	0.7019	0.7326
Dimensionless re-orientation viscosities							
$\tilde{\eta}_{\text{twist1}}$	1.7350	1.6615	1.4450	1.2925	1.2097	0.9897	0.7728
$\tilde{\eta}_{\text{splay}}$	1.3509	1.5459	1.4354	1.2925	1.2081	0.9717	0.7226
$\tilde{\eta}_{\text{bend}}$	1.4713	1.6178	1.4422	1.2925	1.2092	0.9840	0.7557
$\frac{\tilde{\alpha}_3}{\tilde{\eta}_1\,\tilde{\eta}_{\text{splay}}}$	0.284351	0.074746	0.006705	0	0.001373	0.01853	0.06938
Elastic Constants/μdyne							
K_{11}		0.50		0.54		0.69	
K_{33}		0.97		0.45		0.62	

[a]The Leslie viscosities coefficients and the temperature are interpolated values. [b]The average Miesowicz viscosity is defined as: $\langle\eta\rangle = (\eta_1+\eta_2+\eta_3)/3$.

and where the dimensionless average power requirement $\langle\tilde{W}\rangle$ is:

$$\langle\tilde{W}\rangle = \frac{2\pi}{\tilde{\tau}}\int_0^{\tilde{\tau}} \tilde{Q}Er\,\mathrm{d}\tilde{t} \tag{30}$$

Next we establish the relationship between flow alignment and power requirement, and develop a close-form expression that relates P to α_3.

3. Results and discussion

Imposing pressure oscillations on the NLC will produce spatially non-homogeneous director oscillations. Since NLCs are viscoelastic, the director oscillations will not be in-phase with the applied pressure drop. Thus the total director angle $\theta(\tilde{r}, \tilde{t}, \tilde{\omega})$ is given by the sum of the following in-phase, out-phase, and steady components:

$$\theta(\tilde{r}, \tilde{t}, \tilde{\omega}) = \theta_i(\tilde{r}, \tilde{\omega})\sin(\tilde{\omega}\tilde{t}) + \theta_o(\tilde{r}, \tilde{\omega})\cos(\tilde{\omega}\tilde{t}) + \theta_s(\tilde{r}). \tag{31}$$

Note here and in the rest of the paper in-phase means oscillation in-phase with the imposed Ericksen number, and hence the in-phase temporal variation is $\sin(\tilde{\omega}\tilde{t})$, while the out-of-phase is $\cos(\tilde{\omega}\tilde{t})$. Solving equation (31) using separation of variables, the in-phase $\theta_i(\tilde{r}, \tilde{\omega})$, out-of-phase $\theta_o(\tilde{r}, \tilde{\omega})$, and steady $\theta_s(\tilde{r})$ director components are found to be:

$$\theta_i = \frac{\widetilde{\alpha}_3 A E_0}{2\widetilde{\eta}_1}\left(\frac{\mathrm{ber}_1\sqrt{\widetilde{\omega}\widetilde{\eta}_{\mathrm{splay}}}\widetilde{r}\,\mathrm{bei}_1\sqrt{\widetilde{\omega}\widetilde{\eta}_{\mathrm{splay}}} - \mathrm{bei}_1\sqrt{\widetilde{\omega}\widetilde{\eta}_{\mathrm{splay}}}\widetilde{r}\,\mathrm{ber}_1\sqrt{\widetilde{\omega}\widetilde{\eta}_{\mathrm{splay}}}}{\widetilde{\omega}\widetilde{\eta}_{\mathrm{splay}}\left(\mathrm{ber}_1^2\sqrt{\widetilde{\omega}\widetilde{\eta}_{\mathrm{splay}}} + \mathrm{bei}_1^2\sqrt{\widetilde{\omega}\widetilde{\eta}_{\mathrm{splay}}}\right)}\right) \tag{32}$$

$$\theta_{\mathrm{o}} = \frac{\widetilde{\alpha}_3 A E_0}{2\widetilde{\eta}_1}\left(\frac{\mathrm{ber}_1\sqrt{\widetilde{\omega}\widetilde{\eta}_{\mathrm{splay}}}\widetilde{r}\,\mathrm{ber}_1\sqrt{\widetilde{\omega}\widetilde{\eta}_{\mathrm{splay}}} + \mathrm{bei}_1\sqrt{\widetilde{\omega}\widetilde{\eta}_{\mathrm{splay}}}\widetilde{r}\,\mathrm{bei}_1\sqrt{\widetilde{\omega}\widetilde{\eta}_{\mathrm{splay}}}}{\widetilde{\omega}\widetilde{\eta}_{\mathrm{splay}}\left(\mathrm{ber}_1^2\sqrt{\widetilde{\omega}\widetilde{\eta}_{\mathrm{splay}}} + \mathrm{bei}_1^2\sqrt{\widetilde{\omega}\widetilde{\eta}_{\mathrm{splay}}}\right)} - \frac{\widetilde{r}}{\widetilde{\omega}\widetilde{\eta}_{\mathrm{splay}}}\right) \tag{33}$$

$$\theta_{\mathrm{s}} = \frac{\widetilde{\alpha}_3}{\widetilde{\eta}_1}\frac{E_{\mathrm{o}}}{16}\left(1-\widetilde{r}^2\right)\widetilde{r} \tag{34}$$

where $\mathrm{bei}_v(x)$ and $\mathrm{ber}_v(x)$ are the Kelvin functions of order v [22]:

$$\mathrm{ber}_v x = \sum_{k=0}^{\infty}\frac{\cos\left(\frac{3\pi}{4}v + \frac{\pi}{2}k\right)}{k!\Gamma(k+1+v)}\left(\frac{x}{2}\right)^{2k+v} \tag{35}$$

$$\mathrm{bei}_v x = \sum_{k=0}^{\infty}\frac{\sin\left(\frac{3\pi}{4}v + \frac{\pi}{2}k\right)}{k!\Gamma(k+1+v)}\left(\frac{x}{2}\right)^{2k+v}. \tag{36}$$

Since the director field **n** is coupled to the velocity field **v**, see equation (6), imposing an oscillatory pressure drop on the NLC will produce a velocity field with in-phase, out-of-phase, and steady components. Thus the total dimensionless velocity field $\widetilde{v}(\widetilde{r}, \widetilde{t}, \widetilde{\omega})$ is given by the sum of the following in-phase and out-of-phase components:

$$\widetilde{v}\left(\widetilde{r}, \widetilde{t}, \widetilde{\omega}\right) = \widetilde{v}_i(\widetilde{r}, \widetilde{\omega})\sin\left(\widetilde{\omega}\widetilde{t}\right) + \widetilde{v}_{\mathrm{o}}(\widetilde{r}, \widetilde{\omega})\cos\left(\widetilde{\omega}\widetilde{t}\right) + \widetilde{v}_{\mathrm{s}}(\widetilde{r}). \tag{37}$$

As indicated by equation (14), back-flow has a specific contribution to the velocity field through α_3, we can further express the velocity field in terms of pressure drop (ΔP) and back-flow (BF) contributions:

$$\begin{aligned}\widetilde{v}\left(\widetilde{r}, \widetilde{t}, \widetilde{\omega}\right) = {} & \widetilde{v}_{i,\,\Delta P}(\widetilde{r}, \widetilde{\omega})\sin\left(\widetilde{\omega}\widetilde{t}\right) + \widetilde{v}_{\mathrm{o},\,\Delta P}(\widetilde{r}, \widetilde{\omega})\cos\left(\widetilde{\omega}\widetilde{t}\right) + \widetilde{v}_{\mathrm{s},\,\Delta P}(\widetilde{r}) \\ & + v_{i,\,\mathrm{BF}}(r, \widetilde{\omega})\sin(\widetilde{\omega}t) + v_{\mathrm{o},\,\mathrm{BF}}(r, \widetilde{\omega})\cos(\widetilde{\omega}\,t).\end{aligned} \tag{38}$$

Equation (38) shows that back-flow contributes to the in-phase and out-phase velocity components, while pressure drop also has a steady state component $\widetilde{v}_{\mathrm{s},\,\Delta P}(\widetilde{r})$.

Solving equation (14) using separation of variables in conjunction with the director solution, equations (32) and (33), the in-phase ($\widetilde{v}_{i,\,\Delta P}(\widetilde{r}, \widetilde{\omega})$, $\widetilde{v}_{i,\,\mathrm{BF}}(\widetilde{r}, \widetilde{\omega})$), out-of-phase ($v_{\mathrm{o},\,\Delta P}(\widetilde{r}, \omega)$, $v_{\mathrm{o},\,\mathrm{BF}}(\widetilde{r}, \omega)$), and steady $v_{\mathrm{s},\,\Delta P}(\widetilde{r})$ velocity components are found to be:

$$\widetilde{v}_{i,\,\Delta P} = \frac{AE_0}{4\widetilde{\eta}_1}\left(1-\widetilde{r}^2\right);\ \widetilde{v}_{i,\,\mathrm{BF}} = \frac{AE_0}{4}\frac{\widetilde{\alpha}_3^{\,2}}{\widetilde{\eta}_1^2\widetilde{\eta}_{\mathrm{splay}}}\left[\left(1-\widetilde{r}^2\right) + 2F_{vi}\left(\widetilde{\omega}\widetilde{\eta}_{\mathrm{splay}}\right)\right] \tag{39a, b}$$

$$\widetilde{v}_{\mathrm{o},\,\Delta P} = 0;\ \widetilde{v}_{\mathrm{o},\,\mathrm{BF}} = \frac{AE_0}{4}\frac{\widetilde{\alpha}_3^{\,2}}{\widetilde{\eta}_1^2\widetilde{\eta}_{\mathrm{splay}}}\left[2F_{vo}\left(\widetilde{\omega}\widetilde{\eta}_{\mathrm{splay}}\right)\right] \tag{40a, b}$$

$$\widetilde{v}_{\mathrm{s},\,\Delta P}(\widetilde{r}) = \frac{E_0}{4\widetilde{\eta}_1}\left(1-\widetilde{r}^2\right) \tag{41}$$

where the frequency-dependent functions F_{vi}, F_{vo} are:

$$F_{vi}(\widetilde{\omega}\widetilde{\eta}_{\text{splay}}) = \left[\frac{\text{ber}_1\sqrt{\widetilde{\omega}\widetilde{\eta}_{\text{splay}}}\left(\text{ber}_0\sqrt{\widetilde{\omega}\widetilde{\eta}_{\text{splay}}}\widetilde{r} - \text{bei}_0\sqrt{\widetilde{\omega}\widetilde{\eta}_{\text{splay}}}\widetilde{r} - \text{ber}_0\sqrt{\widetilde{\omega}\widetilde{\eta}_{\text{splay}}} + \text{bei}_0\sqrt{\widetilde{\omega}\widetilde{\eta}_{\text{splay}}}\right)}{\sqrt{2\widetilde{\omega}\widetilde{\eta}_{\text{splay}}}\left(\text{ber}_1^2\sqrt{\widetilde{\omega}\widetilde{\eta}_{\text{splay}}} + \text{bei}_1^2\sqrt{\widetilde{\omega}\widetilde{\eta}_{\text{splay}}}\right)}\right] + \left[\frac{\text{bei}_1\sqrt{\widetilde{\omega}\widetilde{\eta}_{\text{splay}}}\left(\text{bei}_0\sqrt{\widetilde{\omega}\widetilde{\eta}_{\text{splay}}}\widetilde{r} + \text{ber}_0\sqrt{\widetilde{\omega}\widetilde{\eta}_{\text{splay}}}\widetilde{r} - \text{bei}_0\sqrt{\widetilde{\omega}\widetilde{\eta}_{\text{splay}}} - \text{ber}_0\sqrt{\widetilde{\omega}\widetilde{\eta}_{\text{splay}}}\right)}{\sqrt{2\widetilde{\omega}\widetilde{\eta}_{\text{splay}}}\left(\text{ber}_1^2\sqrt{\widetilde{\omega}\widetilde{\eta}_{\text{splay}}} + \text{bei}_1^2\sqrt{\widetilde{\omega}\widetilde{\eta}_{\text{splay}}}\right)}\right] \tag{42}$$

$$F_{vo}(\widetilde{\omega}\widetilde{\eta}_{\text{splay}}) = \left[\frac{\text{bei}_1\sqrt{\widetilde{\omega}\widetilde{\eta}_{\text{splay}}}\left(\text{ber}_0\sqrt{\widetilde{\omega}\widetilde{\eta}_{\text{splay}}}\widetilde{r} - \text{bei}_0\sqrt{\widetilde{\omega}\widetilde{\eta}_{\text{splay}}}\widetilde{r} - \text{ber}_0\sqrt{\widetilde{\omega}\widetilde{\eta}_{\text{splay}}} + \text{bei}_0\sqrt{\widetilde{\omega}\widetilde{\eta}_{\text{splay}}}\right)}{\sqrt{2\widetilde{\omega}\widetilde{\eta}_{\text{splay}}}\left(\text{ber}_1^2\sqrt{\widetilde{\omega}\widetilde{\eta}_{\text{splay}}} + \text{bei}_1^2\sqrt{\widetilde{\omega}\widetilde{\eta}_{\text{splay}}}\right)}\right] + \left[\frac{\text{ber}_1\sqrt{\widetilde{\omega}\widetilde{\eta}_{\text{splay}}}\left(\text{bei}_0\sqrt{\widetilde{\omega}\widetilde{\eta}_{\text{splay}}}\widetilde{r} + \text{ber}_0\sqrt{\widetilde{\omega}\widetilde{\eta}_{\text{splay}}}\widetilde{r} - \text{bei}_0\sqrt{\widetilde{\omega}\widetilde{\eta}_{\text{splay}}} - \text{ber}_0\sqrt{\widetilde{\omega}\widetilde{\eta}_{\text{splay}}}\right)}{\sqrt{2\widetilde{\omega}\widetilde{\eta}_{\text{splay}}}\left(\text{ber}_1^2\sqrt{\widetilde{\omega}\widetilde{\eta}_{\text{splay}}} + \text{bei}_1^2\sqrt{\widetilde{\omega}\widetilde{\eta}_{\text{splay}}}\right)}\right] \tag{43}$$

The back-flow contribution has both in-phase and out-of-phase components, and both are proportional to $\widetilde{\alpha}_3^2$. At the flow-aligning transition the back-flow velocities are zero and the flow is Newtonian.

The dimensionless pulsatile flow rate ($\widetilde{Q}$), calculated using equations (25) and (38), is given by:

$$Q(\widetilde{\omega}, \widetilde{t}) = Q_{i,\,\Delta P}(\widetilde{\omega})\sin\widetilde{\omega}\,\widetilde{t} + Q_{\text{o},\,\Delta P}(\widetilde{\omega})\cos\widetilde{\omega}\widetilde{t} + Q_{\text{s},\,\Delta P} + \widetilde{Q}_{i,\,\text{BF}}(\widetilde{\omega})\sin\widetilde{\omega}\widetilde{t} + \widetilde{Q}_{\text{o},\,\text{BF}}(\widetilde{\omega})\cos\widetilde{\omega}\widetilde{t}. \tag{44}$$

The in-phase ($\widetilde{Q}_{i,\,\Delta P}$ and $\widetilde{Q}_{i,\,\text{BF}}$), out-of-phase ($\widetilde{Q}_{\text{o},\,\Delta P}$ and $\widetilde{Q}_{\text{o},\,\text{BF}}$) and steady ($\widetilde{Q}_{\text{s},\,\Delta P}$) flow-rate components are:

$$\widetilde{Q}_{i,\,\Delta P} = \frac{\pi A E_0}{8\widetilde{\eta}_1} \tag{45}$$

$$\widetilde{Q}_{i,\,\text{BF}} = \frac{\pi A E_0}{8\widetilde{\eta}_1}\left(\frac{\widetilde{\alpha}_3^2}{\widetilde{\eta}_1\widetilde{\eta}_{\text{splay}}}\right)\left[1 + 8F_{Qi}(\widetilde{\omega}\widetilde{\eta}_{\text{splay}})\right] \tag{46}$$

$$F_{Qi}(\widetilde{\omega}\widetilde{\eta}_{\text{splay}}) = \left[\frac{\text{ber}_1\sqrt{\widetilde{\omega}\widetilde{\eta}_{\text{splay}}}\left(\frac{1}{2}\text{bei}_0\sqrt{\widetilde{\omega}\widetilde{\eta}_{\text{splay}}} - \frac{1}{2}\text{ber}_0\sqrt{\widetilde{\omega}\widetilde{\eta}_{\text{splay}}}\right)}{\sqrt{2\widetilde{\omega}\widetilde{\eta}_{\text{splay}}}\left(\text{ber}_1^2\sqrt{\widetilde{\omega}\widetilde{\eta}_{\text{splay}}} + \text{bei}_1^2\sqrt{\widetilde{\omega}\widetilde{\eta}_{\text{splay}}}\right)}\right] + \left[\frac{\text{bei}_1\sqrt{\widetilde{\omega}\widetilde{\eta}_{\text{splay}}}\left(-\frac{1}{2}\text{bei}_0\sqrt{\widetilde{\omega}\widetilde{\eta}_{\text{splay}}} - \frac{1}{2}\text{ber}_0\sqrt{\widetilde{\omega}\widetilde{\eta}_{\text{splay}}}\right)}{\sqrt{2\widetilde{\omega}\widetilde{\eta}_{\text{splay}}}\left(\text{ber}_1^2\sqrt{\widetilde{\omega}\widetilde{\eta}_{\text{splay}}} + \text{bei}_1^2\sqrt{\widetilde{\omega}\widetilde{\eta}_{\text{splay}}}\right)}\right] \tag{47}$$

$$\widetilde{Q}_{\text{o},\,\Delta P} = 0 \tag{48}$$

$$\widetilde{Q}_{\text{o},\,\text{BF}} = \frac{\pi A E_0}{8\widetilde{\eta}_1}\left(\frac{\alpha_3^2}{\widetilde{\eta}_1\eta_{\text{splay}}}\right)8\,F_{Q_{\text{o}}}(\omega\eta_{\text{splay}}) \tag{49}$$

$$F_{Qo}(\widetilde{\omega}\widetilde{\eta}_{\text{splay}}) = \frac{\text{bei}_1\sqrt{\widetilde{\omega}\widetilde{\eta}_{\text{splay}}}\left(-\dfrac{2}{\sqrt{2\widetilde{\omega}\,\widetilde{\eta}_{\text{splay}}}}\text{bei}_1\sqrt{\widetilde{\omega}\widetilde{\eta}_{\text{splay}}} - \frac{1}{2}\text{bei}_0\sqrt{\widetilde{\omega}\widetilde{\eta}_{\text{splay}}} + \frac{1}{2}\text{ber}_0\sqrt{\widetilde{\omega}\widetilde{\eta}_{\text{splay}}}\right)}{\sqrt{2\widetilde{\omega}\widetilde{\eta}_{\text{splay}}}\left(\text{ber}_1^2\sqrt{\widetilde{\omega}\widetilde{\eta}_{\text{splay}}} + \text{bei}_1^2\sqrt{\widetilde{\omega}\widetilde{\eta}_{\text{splay}}}\right)} + \frac{\text{ber}_1\sqrt{\widetilde{\omega}\widetilde{\eta}_{\text{splay}}}\left(-\dfrac{2}{\sqrt{2\widetilde{\omega}\,\widetilde{\eta}_{\text{splay}}}}\text{ber}_1\sqrt{\widetilde{\omega}\widetilde{\eta}_{\text{splay}}} - \frac{1}{2}\text{bei}_0\sqrt{\widetilde{\omega}\widetilde{\eta}_{\text{splay}}} - \frac{1}{2}\text{ber}_0\sqrt{\widetilde{\omega}\widetilde{\eta}_{\text{splay}}}\right)}{\sqrt{2\widetilde{\omega}\widetilde{\eta}_{\text{splay}}}\left(\text{ber}_1^2\sqrt{\widetilde{\omega}\widetilde{\eta}_{\text{splay}}} + \text{bei}_1^2\sqrt{\widetilde{\omega}\widetilde{\eta}_{\text{splay}}}\right)} \tag{50}$$

$$\widetilde{Q}_{\text{s},\,\Delta P} = \frac{\pi E_{\text{o}}}{8\widetilde{\eta}_1}. \tag{51}$$

Using equations (26) and (44) the time-average dimensionless flow rate is found to be:

$$\langle\widetilde{Q}\rangle = \widetilde{Q}_i(\widetilde{\omega})\langle\sin\widetilde{\omega}\widetilde{t}\,\rangle + \widetilde{Q}_{\text{o}}(\widetilde{\omega})\langle\cos\widetilde{\omega}\widetilde{t}\,\rangle + \widetilde{Q}_{\text{s}} = \widetilde{Q}_{\text{s}} \tag{52}$$

Equation (52) shows that the average flow rate is $\widetilde{Q}_{\text{s}}$, and thus only the usual pressure drop contribution is present in the linear regime. The energy requirement is given by:

$$\begin{aligned}\langle W\rangle = \langle\widetilde{Q}\;E\rangle = &\left[\widetilde{Q}_{i,\,\Delta P}(\widetilde{\omega}) + \widetilde{Q}_{i,\,\text{BF}}(\widetilde{\omega})\right]E_{\text{o}}\langle\sin\widetilde{\omega}\widetilde{t}(1 + A\sin\widetilde{\omega}\widetilde{t}\,)\rangle \\ &+ \left[\widetilde{Q}_{\text{o},\,\Delta P}(\widetilde{\omega}) + \widetilde{Q}_{\text{o},\,\text{BF}}(\widetilde{\omega})\right]E_{\text{o}}\langle\cos\widetilde{\omega}\widetilde{t}(1 + \text{A}\sin\widetilde{\omega}\widetilde{t}\,)\rangle \\ &+ [Q_{\text{s},\,\Delta P}]E_{\text{o}}\langle 1 + \text{A}\sin\widetilde{\omega}\widetilde{t}\,\rangle\end{aligned} \tag{53}$$

Equations (28), (52) and (53) show that the energy ratio (P) in the linear regime is given by the superposition of the pressure-drop $P_{\Delta P}$ and the back-flow P_{BF} contributions:

$$P = P_{\Delta P} + P_{\text{BF}} \tag{54}$$

Pulsatile flows of liquid crystals have an additional contribution to power requirements. Non-Newtonian fluids that have no coupling between orientation and flow have no back-flow power requirement: $P_{\text{BF}}=0$. Using equations (52) and (53) we find the energy ratio contributions to be:

$$P_{\Delta P} = 1 + \frac{A^2}{2} \tag{55}$$

$$P_{\text{BF}} = \frac{A^2}{2}\left(\frac{\widetilde{\alpha}_3^2}{\widetilde{\eta}_1\widetilde{\eta}_{\text{splay}}}\right)\left[1 + 8F_p(\widetilde{\omega}\widetilde{\eta}_{\text{splay}})\right] \tag{56}$$

where

$$F_P(\widetilde{\omega}\widetilde{\eta}_{\text{splay}}) = \frac{\text{ber}_1\sqrt{\widetilde{\omega}\widetilde{\eta}_{\text{splay}}}\left(\text{bei}_0\sqrt{\widetilde{\omega}\widetilde{\eta}_{\text{splay}}} - \text{ber}_0\sqrt{\widetilde{\omega}\widetilde{\eta}_{\text{splay}}}\right)}{2\sqrt{2}\sqrt{\widetilde{\omega}\widetilde{\eta}_{\text{splay}}}\left(\text{ber}_1^2\sqrt{\widetilde{\omega}\widetilde{\eta}_{\text{splay}}} + \text{bei}_1^2\sqrt{\widetilde{\omega}\widetilde{\eta}_{\text{splay}}}\right)} + \frac{\text{bei}_1\sqrt{\widetilde{\omega}\widetilde{\eta}_{\text{splay}}}\left(-\text{bei}_0\sqrt{\widetilde{\omega}\widetilde{\eta}_{\text{splay}}} - \text{ber}_0\sqrt{\widetilde{\omega}\widetilde{\eta}_{\text{splay}}}\right)}{2\sqrt{2}\sqrt{\widetilde{\omega}\widetilde{\eta}_{\text{splay}}}\left(\text{ber}_1^2\sqrt{\widetilde{\omega}\widetilde{\eta}_{\text{splay}}} + \text{bei}_1^2\sqrt{\widetilde{\omega}\widetilde{\eta}_{\text{splay}}}\right)}. \tag{57}$$

For a liquid crystal it is found that the power requirement scales as $P \propto A^2$, which is in close correspondence to non-Newtonian fluids [20]. Equation (56) is one of the main results of this paper and states that the power requirement due to back-flow scales as:

$$P_{\text{BF}} \propto \widetilde{\alpha}_3^2 \tag{58}$$

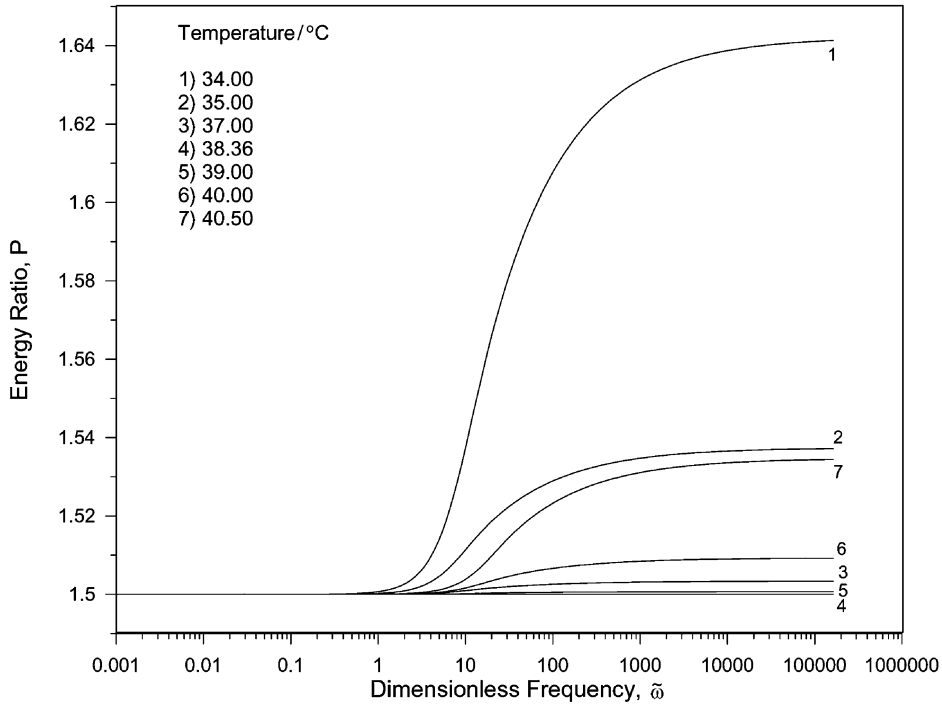

Figure 2. Energy ratio (P) as a function of the dimensionless frequency ($\tilde{\omega}$) for 8CB at different temperatures in the low Ericksen number region and oscillation amplitude $A=1$.

and hence both flow-aligning and non-aligning nematics with the same magnitude of α_3 have the same power requirement.

Figure 2 shows the energy ratio (P) as a function of the dimensionless frequency ($\tilde{\omega}$) for 8CB at different temperatures in the low Ericksen number region, for $A=1$. In the low frequency region the behaviour is Newtonian and $P=1.5$, in agreement with classical results [20]. When the frequency increases the energy ratio increases but this behaviour is temperature-dependent. At the alignment/non-alignment transition temperature ($T=38.36^{\circ}$C) the 8CB displays Newtonian behaviour for all frequencies (line 4). Hence deviation from Newtonian flow increases with the magnitude of α_3. The asymptotic values of equation (45) for low and high frequency are:

$$P_0 = 1 + \frac{A^2}{2} \tag{59}$$

$$P_\infty = 1 + \frac{A^2}{2}\left(1 + \frac{\tilde{\alpha}_3^2}{\tilde{\eta}_1 \tilde{\eta}_{\text{splay}}}\right). \tag{60}$$

In rheological characterization one is interested in universal functions that extract the common features of the response. Typically, the master curve is found by appropriate scaling [3]. In pulsatile flow, a universal energy ratio curve indicates the presence of a frequency-dependent back-flow function. According to equation (54), the energy ratio in the low Ericksen number region can be easily collapsed into a universal curve:

$$P^* = \left[\frac{2}{A^2}(P-1) - 1\right]\frac{\tilde{\eta}_1 \tilde{\eta}_{\text{splay}}}{\tilde{\alpha}_3^2} = 1 + 8F\left(\tilde{\omega}\tilde{\eta}_{\text{splay}}\right) \tag{61}$$

where P^* is the scaled energy ratio. The only parameter remaining in the scaling is

$$\tilde{\omega}\tilde{\eta}_{\text{splay}} = \frac{\omega}{D_{\text{splay}}};\ D_{\text{splay}} = \frac{K_{11}}{R^2 \eta_{\text{splay}}} \tag{62a, b}$$

where D_{splay} is the splay diffusion constant [8–12]. Figure 3 shows the scaled energy ratio as a function of the scaled dimensionless frequency ($\tilde{\omega}\tilde{\eta}_{\text{splay}}$). The function $1+8F\left(\tilde{\omega}\tilde{\eta}_{\text{splay}}\right)$ ranges between 0 and 1 and is a universal rheological liquid crystal function. This function is characterized by an initial 'dead frequency' region ($P^*=0$), an intermediate exponential frequency dependence, and saturation at a large frequency ($P^*\rightarrow 1$). When the ratio of frequency to splay diffusion is close to one, non-Newtonian behaviour sets in and back-flow becomes significant. Equations (54), (59) and (60) show that the scaled energy ratio P^*, see equation (61), can also be given by:

$$P^* = \frac{P - P_0}{P_\infty - P_0}. \tag{63}$$

The universal scaled energy ratio function (P^*) requires the evaluation of the Kelvin functions, see

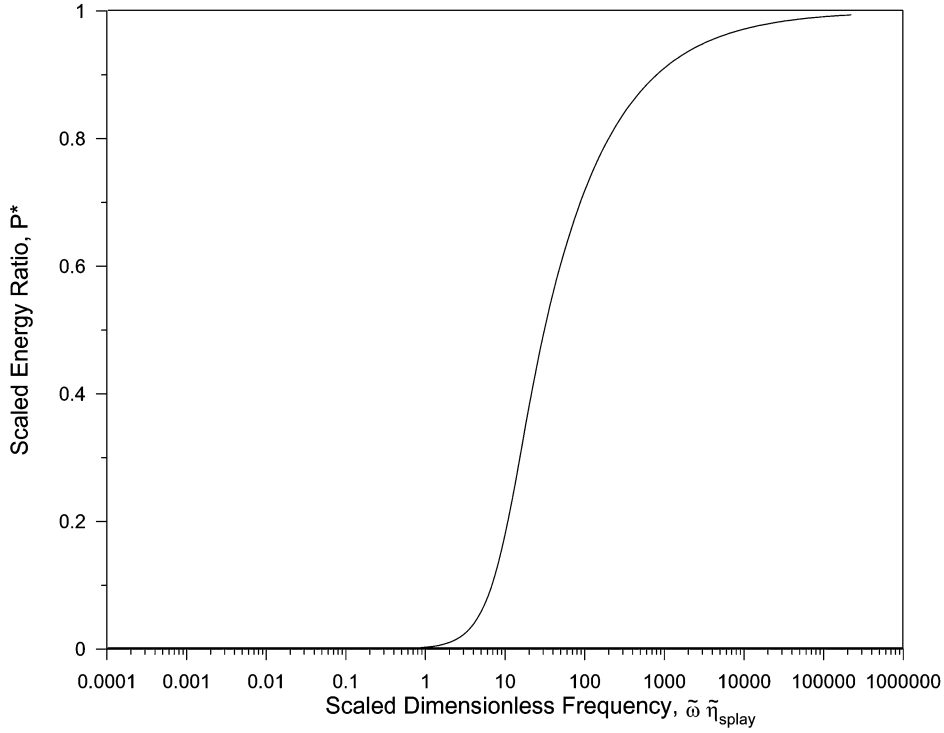

Figure 3. Scaled energy ratio (P^*) as a function of the scaled dimensionless frequency ($\tilde{\omega}\tilde{\eta}_{splay}$). The figure shows that the energy ratio enters an exponential growth when the frequency ω is close to the splay orientation diffusivity D_{splay}, see equation (62*b*). The figure reveals the frequency dependence of back-flow: at small frequencies it is insignificant and at large frequencies it saturates.

equations (35) and (36), and special numerical procedures, not always available. To remove this problem a fitting function was sought and found. The scaled energy ratio P^* was found to be well fitted by:

$$P^* = \frac{1}{1+0.2393\left[\log\left(\tilde{\omega}\tilde{\eta}_{splay}\right)\right]^{-3.40}}. \qquad (64)$$

The two parameters fitting given by equation (64) is almost perfect and the regression coefficient (R^2) is 0.99998.

Having found a characteristic back-flow function, next we establish how best to extract qualitative and quantitative flow-alignment information from a pulsatile flow. According to equation (60), the large frequency limit of the energy ratio P_∞ provides a way to extract α_3 from power measurements. Figure 4 shows the large frequency value energy ratio P_∞, see equation (66), as a function of viscosity coefficient α_3 for 8CB. The figures shows that Newtonian behaviour is found at the aligning/non-aligning transition temperature ($T=38.36^\circ$C) that corresponds to $\alpha_3=0$. The figure shows that the power requirement decreases with decreasing temperature if the material is non-aligning, and increases with decreasing temperature if it is aligning. Hence a few measurements at several temperatures reveal whether the material is aligning or not. Furthermore the deviation from $P=1.5$ reveals a deviation of α_3 from $\alpha_3=0$. Many liquid crystalline polymers have values of α_3 close to zero, and pulsatile flow may provide another way to verify this important parameter. In a rheological experiment, the frequency at which back-flow sets in gives the splay viscosity:

$$\eta_{splay} = \frac{K_{11}}{R^2\omega_{exp}}. \qquad (65)$$

Measurement of the power ratio at large frequencies with a known amplitude A, allows one to compute the flow-alignment coefficient α_3:

$$\alpha_3 = \left\{\left(\frac{2(P_\infty-1)}{A^2}-1\right)\frac{\eta_1 K_{11}}{R^2\omega_{exp}}\right\}^{\frac{1}{2}} \qquad (66)$$

if the capillary radius R, the Miesowicz viscosity η_1, and the splay Frank constant K_{11} are known.

4. Conclusions

This paper presents analytical solutions to the capillary pulsatile flow of Leslie–Ericksen liquid crystals under

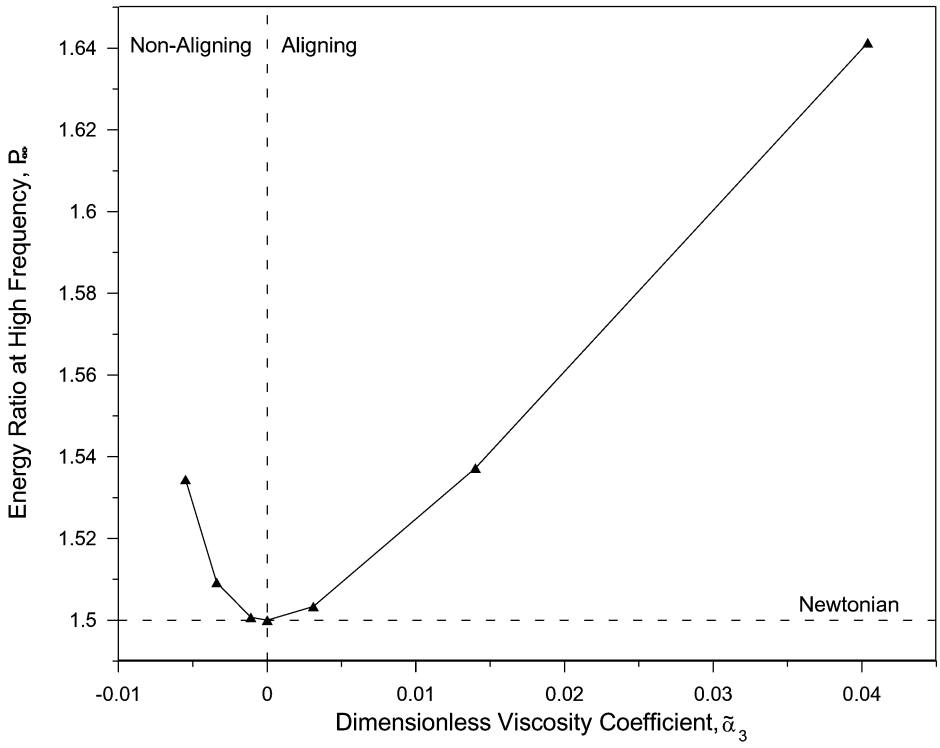

Figure 4. Asymptotical large frequency value of the energy ratio (P_∞) as a function of the dimensionless viscosity coefficient ($\tilde{\alpha}_3$), computed for 8CB, see table I and equation (60). The minimum in the parabola corresponds to the aligning-non-aligning rheological transition. Measurements of P in conjunction with the transition frequency ($\omega = D_{\text{splay}}$) shown in figure 3 provide a means to evaluate α_3.

small pressure drops. The analytical results are used to compute the power requirement in terms of frequency and amplitude of the pulsating pressure drop and in terms of viscoelastic material parameters. Pulsatile flows are useful in measuring rheological material functions because periodic perturbations to a steady flow create periodic back-flows. The analysis reveals that power requirements deviate from Newtonian behaviour when the frequency of the oscillating pressure drop is close to the splay orientation diffusivity and backflows become significant. At small frequencies the response is Newtonian and the power requirement is a quadratic function of amplitude. At large frequencies, the amplitude of back-flow effects saturates and the power requirement is proportional to the square of the alignment viscosity coefficient α_3. The frequency dependence of the back-flow is a universal function and can be expressed with a simple logarithmic expression. An experimental procedure to measure the alignment viscosity coefficient α_3 is formulated, based on the large frequency measurements, and a theoretical expression derived from the close-form solution to pulsatile flow of Leslie–Ericksen liquid crystals.

Acknowledgements

This research was supported by the Engineering Research Centers Program of the National Science Foundation under NSF Award Number EEC-9731680.

References

[1] P.G. de Gennes, J. Prost. *The Physics of Liquid Crystals* 2nd Edn, Oxford University Press, London (1993).
[2] A.D. Rey, M.M. Denn. *Ann. Rev. Fluid Mech.*, **34**, 233 (2002).
[3] R.G. Larson. *The Structure and Rheology of Complex Fluids*. Oxford University Press, New York (1999).
[4] R.B. Bird, R.C. Armstrong, O. Hassager. *Dynamics of Polymeric Liquids*. John Wiley, New York (1989).
[5] K. Walters. *Rheometry*. Wiley, New York (1975).
[6] T. Carlsson. *J. de Physique (Paris)*, **44**, 909 (1983).
[7] W.H. Han, A.D. Rey. *J. Rheol.*, **39**, 301 (1995).
[8] L.R.P. de Andrade Lima, A.D. Rey. *J. Rhel.*, **47**, 1261 (2003).
[9] L.R.P. de Andrade Lima, A.D. Rey. *Chem. Eng. Sci.*, **59**, 3891 (2004).
[10] L.R.P. de Andrade Lima, A.D. Rey. *Phys. Rev. E*, **70**, 011701:1 (2004).
[11] L.R.P. de Andrade Lima, A.D. Rey. *J. Rheol.*, **48**, 1067 (2004).

[12] L.R.P. de Andrade Lima, A.D. Rey. *Rheol Acta* (in the press) DOI: 10.1007/500397-005-0003-0. (2005).
[13] P.T. Mather, D.S. Pearson, R.G. Larson, D.F. Gu, A.M. Jamieson. *Rheol. Acta*, **36**, 485 (1997).
[14] W.H. Han, A.D. Rey. *J. Rheol.*, **38**, 1317 (1994).
[15] W.H. Han, A.D. Rey. *Phys. Rev. E*, **50**, 1688 (1994).
[16] F.R.S. Chandrasekhar. *Liquid Crystals* 2nd Edn, Cambridge University Press, (1992).
[17] H. Kneppe, F. Schneider, N.K. Sharma. *Ber. Bunsenges. Phys.Chem.*, **85**, 784 (1981).
[18] H. Kneppe, F. Schneider, N.K. Sharma. *J. chem. Phys.*, **77**, 3203 (1982).
[19] H.A.M. Barnes, P. Townsend, K. Walters. *Rheol. Acta*, **10**, 517 (1971).
[20] M.F. Edwards, D.A. Nellist, W.L. Wilkinson. *Chem. Eng. Sci.*, **27**, 545 (1972).
[21] L.R.P. de Andrade Lima, A.D. Rey. *Chem. Eng. Sci.*, **60**, 6622 (2005).
[22] M. Abramowitz, I.A. Stegun. *Handbook of Mathematical Functions*. Dove Publications, New York (1972).